

Comparison of the Ballistic Performance of Kevlar and UHMWPE Helmets Using FEM

I.F. Saruhan^{#,*} and R. Gunes[§]

[#]Center of Research CES Advanced Composites and Defence Technologies, Ankara, Turkey

[§]Department of Mechanical Engineering, Erciyes University, Kayseri, Turkey

*E-mail: furkan.saruhan.5306@gmail.com

ABSTRACT

This numerical study compares the ballistic performance of Kevlar and UHMWPE (Ultra-High Molecular Weight Polyethylene) helmets. Armor models were obtained from experimental, numerical, and analytical studies in the literature, as well as the mechanical properties of Kevlar and UHMWPE were also obtained from the literature. Ballistic limit studies were performed to verify the materials. The residual velocities of FSPs fired at Kevlar and UHMWPE plates were compared with experimental data in the literature for Kevlar and the error rate was found to be 4.64 %. The UHMWPE ballistic limit converged to the analytical model in the literature with an error rate of 1 %. After the validation of the models, the ballistic performance of the helmets was analysed according to the NIJ 0106.01 standard. The pressure changes, pressure distributions, and positions of Kevlar and UHMWPE helmets under ballistic impact are shown. In addition, composite damages and Back Face Deformations (BFD) of the helmets were calculated. Kevlar ballistic helmet BFD value was 16.9 mm, while UHMWPE ballistic helmet BFD value was 18.8 mm. Thus, the ballistic protection performance and ballistic impact mechanisms of the helmets were analysed. While both helmets were found to provide NIJ II level protection, the fibre and matrix damage in the Kevlar helmet was higher than those of the UHMWPE helmet, but the BFD causing trauma was lower than those of the UHMWPE helmet. However, when the density of the UHMWPE helmet is considered, it is effectively lighter than the Kevlar helmet. In this study, numerical models of Kevlar and UHMWPE helmets were introduced to the literature and a study comparing their ballistic protection effects was conducted and the results are intended to guide future designs.

Keywords: Ballistic helmets; Finite element method; Protection mechanisms; Kevlar; UHMWPE

NOMENCLATURE

V_{50} : Ballistic limit velocity
 V_r : Residual velocity
FSP : Fragment simulating projectile
FMJ : Full metal jacket

1. INTRODUCTION

Modern helmets are a type of wearable armour that protects the head area of military personnel in conventional warfare situations and asymmetric military conflicts, but they must provide ballistic protection against ballistic threats, fast particles, and explosions¹. The head and neck area causes 12 % of a person's body. Traumatic Brain Injury (TBI) caused by a threat hitting this area is the cause of death and disability in modern conflicts¹. According to the Defence and Veterans Brain Injury Centre (DVBIC), 444,328 TBIs were recorded between 2000 and 2021². Modern helmets should be designed in such a way that many communication technologies can be used on them as well as high protection level, lightness, and comfortable use. In helmet design, critical issues such as materials, ballistic impact mechanisms, manufacturing, performance, and protection against head injuries need to be addressed. Modern helmets are manufactured from high-

strength, lightweight composite materials that have proven themselves as ballistic protection. There are basically two main materials, KEVLAR and UHMWPE fibres¹.

Since the First World War, many helmets have been designed against ballistic threats and high-speed fragments. According to research, US military forces used helmets made of M1 steel from the 1940s to the late 1970s. These highly rigid helmets could provide some ballistic protection, but they were heavy and uncomfortable and offered little protection from blunt trauma³. Kevlar, produced by Stephanie Kwolek and patented by DuPont, has started to be used as a ballistic material due to its high strength, lightweight and high toughness properties⁴. After Kevlar proved itself as a ballistic material, PASGT (Personel Armour System for Ground Troops) emerged as the first helmet made of composite materials in the mid-1980s^{1,3-4}. The PASGT helmet evolved into the lighter MICH (Modular Integrated Communications Helmet) helmet, on which integrated communication systems are placed.

Since the 2000s, ACH (Advanced Combat Helmet) has been used as the primary helmet by the USA^{1,3}. Recently, with the development of material technology, UHMWPE (ultra-high molecular weight polyethylene) composite has taken its place in ballistic applications due to its very good ballistic performance along with its strength and mass performance^{1,4}. Thermoplastic-based UHMWPE has attracted great interest

in military armour applications due to its high fibre strength and low weight. With the introduction of UHMWPE in combat helmets, ECH (Enhanced Combat Helmet) helmets have emerged and it has been determined that the high-speed particle protection rate is at least 37 % higher than ACH, a Kevlar-based helmet⁵.

Analyses of ballistic mechanisms are extremely complicated. Numerical, analytical, and experimental studies can be carried out for these analyses, as well as a combined approach. In the following paragraphs, examples of these analyses in the literature will be described.

An article presents a comparative study on the design, materials, and ballistic performance of combat helmets used by the US Army. Curvature was found to have a significant effect on the ballistic limit of the composite helmet⁶. The ballistic performance of the Advanced Combat Helmet was evaluated numerically and experimentally. The studies were carried out according to the requirements of the NIJ-0106.01 standard. Simulations were also carried out together with experimental studies. A 9 mm projectile and a 1.1 g Fragment Simulating Projectile (FSP) were used in the study. In the simulation, the helmet was subjected to ballistic resistance testing, and the predicted Back Surface Deformations (BFD) were shown to be consistent with the test data⁷. In another study, the response of Aramid composite helmet shells under the ballistic effect of FSP and Full Metal Jacketed Projectiles was analysed by simulations. Experimental studies on composite plates and ballistic tests on the helmet provided real data, which were compared with model predictions and the accuracy of the developed numerical models was proved⁸. In another study, a finite element (FE) model of a Kevlar helmet and head was created. The data obtained from FE simulations are biomechanical behaviours such as stress in the skull bone and strain in the brain tissue. According to the literature, compact cranial bone fractures are observed at 48-128 MPa in tension and cancellous bone fractures at 32-74 MPa in compression⁹. Explains that injuries can occur with blunt trauma caused by a helmet BFD. Possible resulting injuries include skull fracture, haematoma, concussion, contusion, diffuse axonal injury, etc. In one study, helmet performance testing methodology was developed using digital imaging¹⁰. In another trauma study, finite element analysis was used to optimize composite helmets taking into account biomechanical requirements. The results of high-speed impacts of a human head protected by an aramid combat helmet under the ballistic limit were analysed¹¹. In one study, the impact response of a composite structure consisting of a metal-filled ceramic interlayer and UHMWPE laminate was investigated through ballistic testing and numerical simulation¹². In another study, a finite element model was developed to predict the behaviour of UHMWPE fibre composite laminates under impact loading. Detailed views of fracture modes and delamination patterns in composite layers were obtained and analysed¹³.

Studies to date have shown that modern ballistic helmets no longer show full penetration, and provide protection according to the NIJ 0106.01 standard. However, blunt trauma is still a serious problem. It is very important to design lightweight and reliable helmets that fully protect military personnel from the

effects of trauma. For this reason, new materials with advanced technology have started to be used. These materials are Kevlar and UHMWPE fibres. Some countries or associations around the world still use Kevlar ballistic helmets. The ballistic performance of Kevlar has been analysed experimentally and numerically both as a plate and as a helmet. However, although there are studies on the plates of UHMWPE composites, there is no analysis of a ballistic helmet in the literature. There are many differences between the impact mechanics of ballistic helmets and the impact mechanics of plates. Curvilinear surfaces are the most obvious difference of helmets and at the same time protect the most critical part of the human body. In this study, the ballistic behaviour of Kevlar 129 and UHMWPE plates was verified by studies in the literature. A new model was created for the ballistic helmet made of Kevlar 129 composite, which has high ballistic performance and is still in use. In addition, UHMWPE ballistic helmets consisting of very low-density and strong fibres, which have become widespread in the world, have also been numerically modeled for the first time and introduced to the literature. The behaviours of both modeled helmets under the ballistic impact, their protection effects, weight parameters, and pressure responses due to impact were revealed and compared. Pressure generation at the moment of impact, its locations, and its distribution along the impact were observed. BFD and composite damages on the helmets were analysed and the advantages and disadvantages of both advanced helmets were discussed. It is thought that the comparison of the protection mechanisms of the numerical helmet models introduced to the literature in the same study will shed light on future studies and will be an effective resource for designers.

2. METHODOLOGY

Numerical methods and programmes can be used to explain and analyse mechanics such as ballistics, impact and fall. Very complex problems can be solved and mechanics can be explained with software programmes¹⁴. Recognised and universally accepted standards are used to assess ballistic performance. These are the NIJ 0106.01 and STANAG V_{50} ballistic standards. Here, the NIJ standard can be summarised as a pass-or-fail test. A shot is fired at the helmet, which is attached to a head form, from a certain distance. Chronograph between the helmet and the barrel, the bullet speed can be measured. Thus, the protection level of the helmet can be determined depending on the standard bullet and its speed. The amount of deformation in the helmet after the shot can be measured. The protection status against dynamic high-velocity impacts related to the identified threats is examined¹⁵. NIJ standard threat types and speeds are given in Table 1. The helmet geometry subjected to NIJ tests in this study is as given in Fig. 1.

NATO STANAG 2920 standard focuses on the V_{proof} (Ballistic Limit) and V_{50} ballistic tests and the national authorities can define the minimum V_{proof} according to the technical specifications of armor or ballistic protection materials. The main factor in defining the V_{proof} and V_{50} velocity is the risk analysis of national authority. NATO STANAG 2920 standard gives an opportunity to have a protection against different

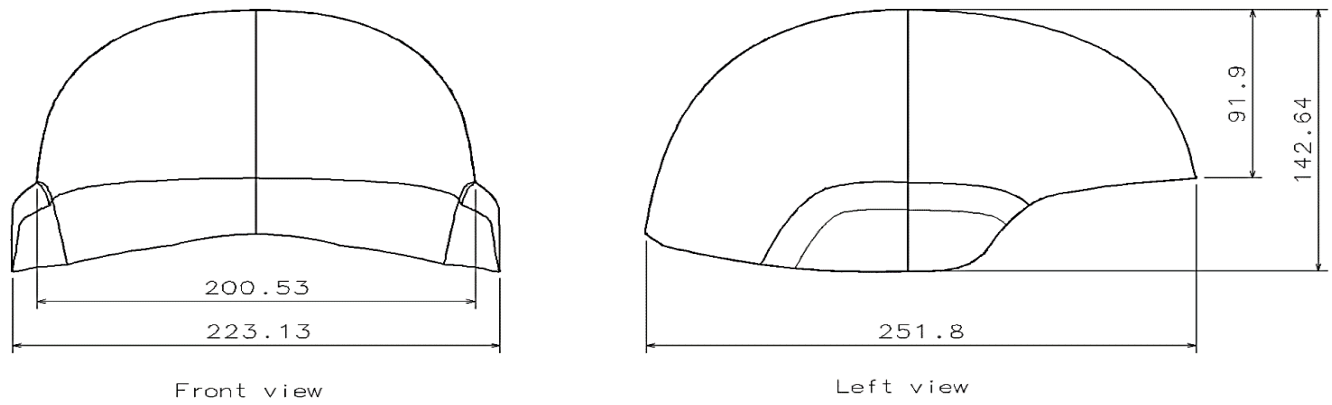


Figure 1. Helmet dimensions (all dimensions are in mm).

Table 1. NIJ 0106.01 standard¹⁵

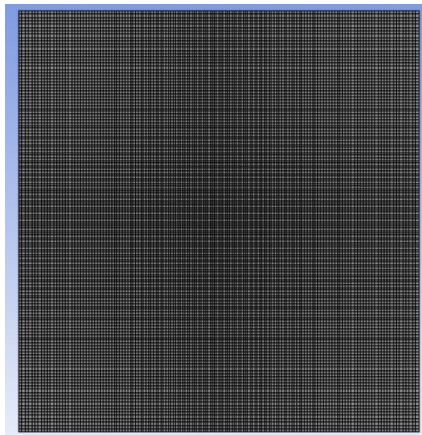
Protection level	Threat	Weight (g)	Velocity (m/s)
I	22 LRHV	2.6	320 ± 12
	38 Special RN	10.2	259 ± 15
II-A	357 Magnum	10.2	381 ± 15
	9 mm FMJ	8	332 ± 15
II	357 Magnum	10.2	425 ± 15
	9 mm FMJ	8	358 ± 15

residual velocity values of the threat can be calculated.

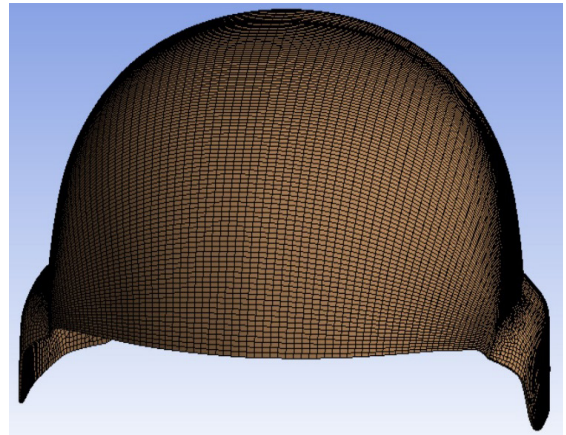
$$V_{res} = a(V_{imp}^p - V_b^p)^{1/p} \tag{1}$$

$$V_{imp} > V_b \tag{2}$$

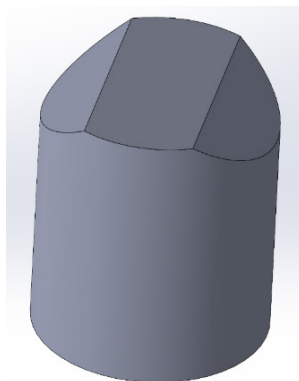
Here, V_{imp} is the impact velocity of the projectile, V_{res} is the residual velocity after the projectile pierces the plate and V_b is the ballistic limit velocity. a and p are the coefficients obtained from experimental data and when $p=2$, the equation is called Recht-Ipson approximation.



(a)



(b)



(c)



(d)

Figure 2. (a) Finite element models of the plate; (b) Finite element model of the ballistic helmet; (c) Model of the Fragment Simulating Projectile (FSP) (STANAG); and (d) Model of the Full Metal Jacket (FMJ) bullet (NIJ)

projectiles and different V_{proof} and V_{50} threat levels based on the risk analysis of the national authority on the armor¹⁶.

Another approach to the ballistic limit concept is the Lambert-Jonas approach. With this analytical approach, the

$$V_{res} = a(V_{imp}^2 - V_b^2)^{1/2} \tag{3}$$

$$a = \frac{M}{(M + m)} \tag{4}$$

M, is the mass of the projectile and m is the mass of the fragment broken off from the projectile by the impact.

In other words, when $V_{res}=0$, the impact velocity V_{imp} is equal to the ballistic limit velocity V_{bl} ¹⁷.

In this study, threats and armours were modeled in Solidworks. The composite modeling was performed in ANSYS/ACP and LS-DYNA was used as solver.

Before evaluating the ballistic performance of the helmets, STANAG V_{50} and residual velocity (V_{res}) studies were carried out on Kevlar and UHMWPE plates and the results were tried to converge with the literature.

STANAG V_{50} test was performed for Kevlar plates. For this standard, the bullet was selected as FSP (.22 cal) and convergence to the literature was attempted.

For UHMWPE plates, a 20 mm FSP projectile was used and residual velocities (V_{res}) were determined and verified with the literature.

FMJ (8 g) bullet was used in ballistic tests for helmets according to NIJ standards. MAT_RIGID material model is defined as a material model for threats.

For mesh optimisation, shots were made on helmets with different mesh sizes. The study was performed for both Kevlar and UHMWPE helmets. The amount of BFD occurring after the shot was considered accurate to the extent that the mesh-dependent results varied negligibly. The results are given in Table 2.

Table 2. Mesh optimisation study for helmets

Mesh size (mm)	BFD of Kevlar Helmet (mm)	BFD of UHMWPE helmet (mm)
4	15.7	14.7
2	17.2	15.2
1	16.9	18.8
0.5	17.0	19.0

The finite element models shown in Fig. 2 were optimised by performing many ballistic tests. There are 23,808 elements in the plate and 15,363 elements in the helmet. The mesh size was determined as 1 mm with the parametric shooting trials. Here, the results do not change in sizes below 1 mm mesh size. Here, the plates were fixed from the edges, while the helmets were fixed from the lower edges of the ear parts. The reason for this is both because it is connected to the fixture from the connection apparatus in the ears in the standard and because it is the region that will affect the analysis result the least.

Ballistic helmets were modeled with 15 layers and 6.8 mm in thickness. The composite plates to be used for STANAG 2920 tests were modeled as 20 layers with shell elements in ANSYS/ACP.

The same material model and solution equations were used for both armours.

MAT_ENHANCED_COMPOSITE_DAMAGE material model was used as the material model. The contact relationship between the threat and the armor was defined with the ERODING_SURFACE_TO_SURFACE contact algorithm. In numerical analysis, the 5. type HOURGLASS based on the Flanagan-Belytschko stiffness form is defined to avoid non-physical deformations in composite plates. The mechanical

properties given in Table 3 are defined when modeling composite armours.

The macroscopic representation of UHMWPE laminates is orthotropic. For this orthotropic material, its constitutive relation can be expressed as:

$$\begin{Bmatrix} \varepsilon_1 \\ \varepsilon_2 \\ \varepsilon_3 \\ \gamma_{23} \\ \gamma_{13} \\ \gamma_{12} \end{Bmatrix} = \begin{bmatrix} \frac{1}{E_1} & -\nu_{12} & -\nu_{13} & 0 & 0 & 0 \\ \frac{-\nu_{12}}{E_2} & \frac{1}{E_2} & -\nu_{23} & 0 & 0 & 0 \\ \frac{-\nu_{13}}{E_3} & -\nu_{23} & \frac{1}{E_3} & 0 & 0 & 0 \\ 0 & 0 & 0 & \frac{1}{G_{23}} & 0 & 0 \\ 0 & 0 & 0 & 0 & \frac{1}{G_{13}} & 0 \\ 0 & 0 & 0 & 0 & 0 & \frac{1}{G_{12}} \end{bmatrix} \begin{Bmatrix} \sigma_1 \\ \sigma_2 \\ \sigma_3 \\ \tau_{23} \\ \tau_{13} \\ \tau_{12} \end{Bmatrix} \quad (5)$$

where, E, G, ν were the elastic modulus, shear modulus, and Poisson ratio of the composite laminate, respectively, and the subscripts 1, 2, and 3 denoted local element axes. The mechanical properties used in the equation solutions are shown in Table 3. Equation definitions for the material card MAT 54 used for composite damages are as follows¹²:

For the tensile fiber mode,
 $\sigma_{aa} > 0$ then

$$e_f^2 = \left(\frac{\sigma_{aa}}{X_t}\right)^2 + \beta \left(\frac{\sigma_{ab}}{S_c}\right)^2 - 1 \begin{cases} \geq 0 & \text{failed} \\ < 0 & \text{elastic} \end{cases} \quad (6)$$

$$E_a = E_b = G_{ab} = \nu_{ba} = \nu_{ab} = 0 \quad (7)$$

For the compressive fiber mode,

$\sigma_{aa} < 0$ then

$$e_c^2 = \left(\frac{\sigma_{aa}}{X_c}\right)^2 - 1 \begin{cases} \geq 0 & \text{failed} \\ < 0 & \text{elastic} \end{cases} \quad (8)$$

$$E_a = \nu_{ba} = \nu_{ab} = 0 \quad (9)$$

For the tensile matrix mode,

$\sigma_{bb} > 0$ then

$$e_m^2 = \left(\frac{\sigma_{bb}}{Y_t}\right)^2 + \beta \left(\frac{\sigma_{ab}}{S_c}\right)^2 - 1 \begin{cases} \geq 0 & \text{failed} \\ < 0 & \text{elastic} \end{cases} \quad (10)$$

$$E_a = \nu_{ba} = 0 \rightarrow G_{ab} = 0 \quad (11)$$

Table 3. Mechanical properties of Kevlar 129 and UHMWPE¹⁰⁻¹¹

Mechanical properties	Kevlar 129	UHMWPE (Dyneema HB 26)
Density(kg/m ³)	1230	970
E_1 (GPa)	18.5	34.257
E_2 (GPa)	18.5	34.257
E_3 (GPa)	6	3.26
G_{12} (GPa)	0.77	0.1738
G_{23} (GPa)	2.5	0.5478
G_{13} (GPa)	2.5	0.5478
ν_{12}	0.25	0
ν_{23}	0.33	0.013
ν_{13}	0.33	0.013

For the compressive matrix mode, $\sigma_{bb} > 0$ then

$$e_d^2 = \left(\frac{\sigma_{bb}}{2S_c}\right)^2 + \left[\left(\frac{Y_c}{2S_c} - 1\right)^2 - 1\right] \frac{\sigma_{bb}}{Y_c} + \left(\frac{\sigma_{ab}}{S_c}\right)^2 - 1 \begin{cases} \geq 0 & \text{failed} \\ < 0 & \text{elastic} \end{cases} \quad (12)$$

$$E_b = v_{ba} = v_{ab} = 0 \Rightarrow \begin{matrix} G_{ab} = 0 \\ X_c = 2Y_c \end{matrix} \quad (13)$$

3. RESULTS & DISCUSSIONS

At the beginning of the helmet analysis, the mechanics of UHMWPE and Kevlar armours were investigated by converging numerical, experimental, and analytical studies in the literature to examine the solution capabilities of the program for the case to be studied and to ensure the accuracy of the ballistic helmet modeling.

Firstly, studies on Kevlar and UHMWPE plates were identified to validate the models. Ballistic limit and residual velocity studies of Kevlar and UHMWPE plates were taken from separate papers and validated for their respective cases.

A ballistic helmet was modeled with the validated material models and programme solving capability. This helmet was modeled as both Kevlar and UHMWPE armour and tested according to NIJ standards. The aim here is to compare the ballistic protection mechanisms of Kevlar and UHMWPE helmets. In this study, the advantages and disadvantages of both helmets compared to each other are presented numerically, and while presenting this situation, it is aimed to provide a validated UHMWPE helmet model to the literature.

3.1 Ballistic Limit Study for Kevlar Plate

The ballistic limit study is statistical. In V_{50} tests, which are subject to STANAG standards, a minimum of six shots are fired with a fragment simulating projectile. The three highest velocities at which the armour cannot be penetrated and the three lowest velocities at which the fragment can penetrate the armour are averaged¹⁸. A numerical approximation to an experimental V_{50} test in the literature was attempted for the modeling and validation of Kevlar plates. The ballistic limit value of the plate was investigated by firing 0.22 cal FSP at different velocities to Kevlar plates measuring 400×400×9.1 mm. The results were recorded as full penetration and partial penetration. CP (Full Penetration) and PP (Partial Penetration) means. The limit where the armour completely absorbs the energy of the threat and the remaining velocity is very low is accepted as the ballistic limit. Table 4 shows the data of the experimental ballistic limit study in which full penetration (CP) and Partial Penetration (PP) cases were observed at different ballistic impact velocities. An average velocity value was taken from the experimental study and as a result, the ballistic limit was estimated. This estimate is 686.6 m/s⁸.

As shown in Table 4, a large number of shots were fired at the model prepared for numerical simulations. Velocities were increased at 10 m/s intervals. Ballistic limit calculation was performed and high convergence was achieved with experimental ballistic limit studies. In the numerical study, the

Table 4. Experimental ballistic limit studies in the literature⁸ and the ballistic limit calculation performed in this study

Ballistic impact	Velocity (m/s)	CP	PP	
1	696.3	√		Experimental V_{50} in the literature (± 30 m/s) 686.6
2	691.5	√		
3	658.5		√	
4	665.6		√	
5	692.2		√	
6	703.7	√		
7	670.2			
Ballistic impact	Velocity (m/s)	CP	PP	
1	680		√	Ballistic limit in this study (± 10 m/s) 720
2	690		√	
3	700		√	
4	710		√	
5	720	√		
6	730	√		
7	740	√		

ballistic limit was found to be 720 ± 10 m/s. Here, the crossing of the FSP at very low speeds is accepted as CP, while the FSP cannot cross completely and turns back is accepted as PP. In PP cases, damage was observed on the plates in collisions at speeds close to the ballistic limit.

When the ballistic impact occurred at 720 m/s, the residual velocity was calculated very low (almost zero). The armor could not be penetrated in the ballistic impact performed 10 m/s below this velocity, and the armor was completely penetrated in the ballistic impact performed above 10 m/s. The error rate between the numerical analysis and the literature study⁸ was found to be 4.64 %.

Figure 3 shows the over time pressure distributions resulting from the impact of 0.22 cal FSP at 720 m/s on the Kevlar plate. The instantaneous pressure that starts as a point starts to spread in the fibre directions and when the pressure reaches the plate boundaries, it is distributed over the entire surface. When the threat passes to the back surface of the armour and breaks contact, the pressure decreases over time.

3.2 Residual Velocity Study of UHMWPE

Residual velocity is the velocity of the threat after it hits the armour and causes full penetration. This velocity is related to how much the armour can absorb the energy of the threat. To determine the energy absorption capacity of UHMWPE armour and to verify the prepared model, the study was carried out using data from previous numerical and analytical models in the literature.

The projectile used for the analysis here is a FSP made of 4340 steel with a diameter of 20 mm and a mass of 54 g. A UHMWPE plate measuring 300×300×10 mm was used for ballistic test analysis. In this study, convergence to a previous numerical simulation study¹⁹ and the Lambert-Jones analytical model is attempted. The initial velocities and residual velocities of the FSP were evaluated in the study.

As shown in Table 5, the numerical ballistic analysis results are consistent with the analytical results. For the study, four

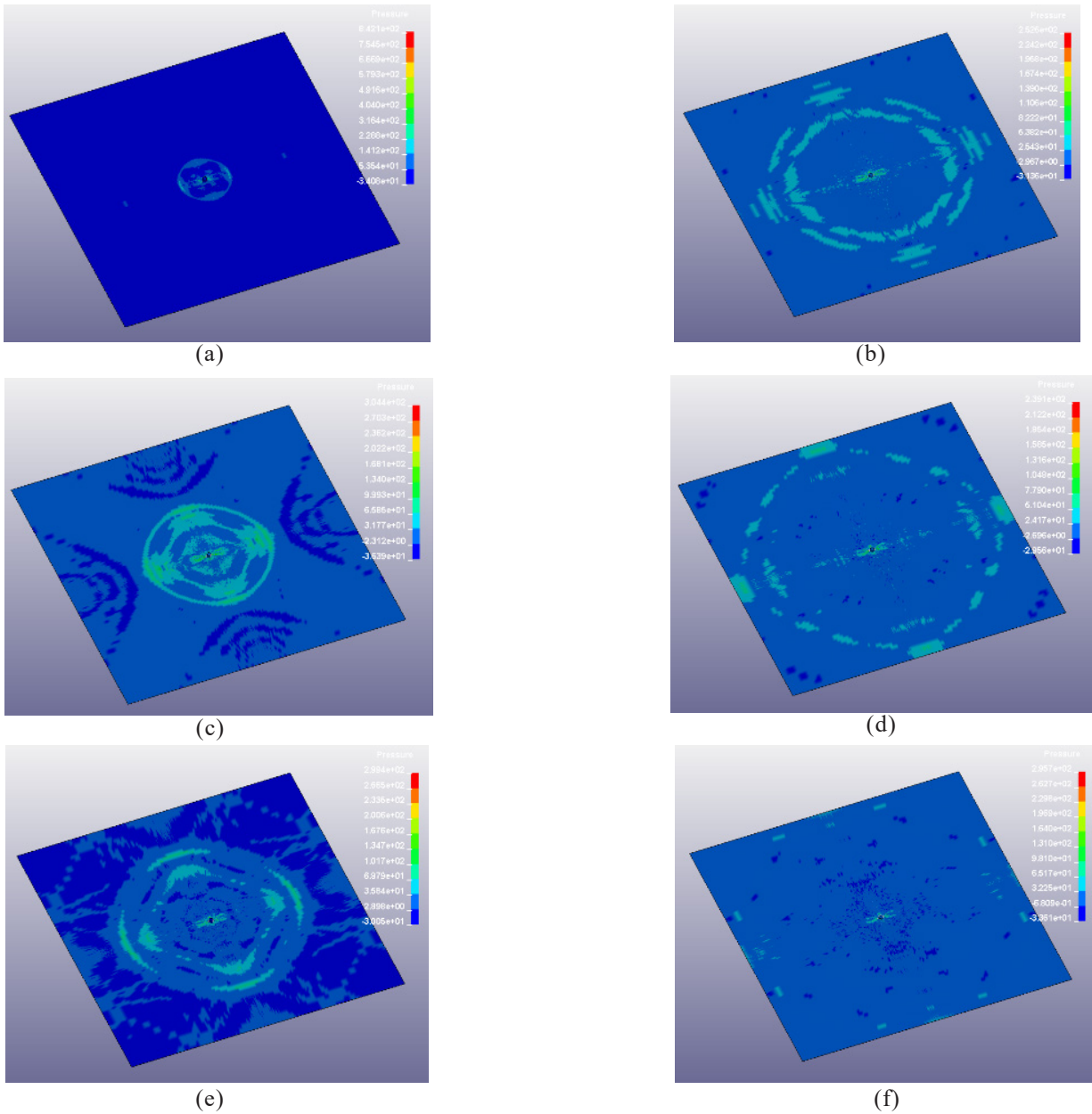


Figure 3. Variation of pressure distribution in Kevlar plates over time; (a) $t = 0.0000425$ s; (b) $t = 0.0000169$ s; (c) $t = 0.000085$ s; (d) $t = 0.0000254$ s; (e) $t = 0.0000127$ s; and (f) $t = 0.0000297$ s.

Table 5. Comparison of the V_{res} residual velocities obtained from this study with numerically founded in the literature and analytically calculated V_{res} residual velocity values¹⁹

Ballistic impact velocities (m/s)	Lambert-Jones analytical equation V_{res} (m/s)	This study V_{res} (m/s)
425	197.75	227
443	243	244
470	297.95	268
648	553.65	521

shots were fired at different velocities, and residual velocities were determined. After four shots, Lambert-Jones converged to the analytical equation with an average error rate of 1 %. As a result of this study, the model should be considered to be highly accurate. Figure 4 shows the time-dependent pressure distributions on UHMWPE plates as a result of the impact of

a 20 mm FSP with a speed of 648 m/s on the UHMWPE plate. The high caliber FSP hits the plate well above the ballistic limit velocities. While the instantaneous pressure generated at the impact point spreads, pressure build-up is also observed at the support points.

3.3 Ballistic Performance of Kevlar and UHMWPE Helmets

Here, the performance of ballistic helmets has been tested and compared according to the NIJ II level. 9 mm parabellum (8 g) threats were fired at 358 m/s into the front of the ballistic helmets. The performance of Kevlar and UHMWPE ballistic helmets of the same geometry and thickness was analysed.

The back surface deformation causing head trauma is defined as dynamic deformation. The armour, which moves with the threat for a while, tries to return to its old geometry

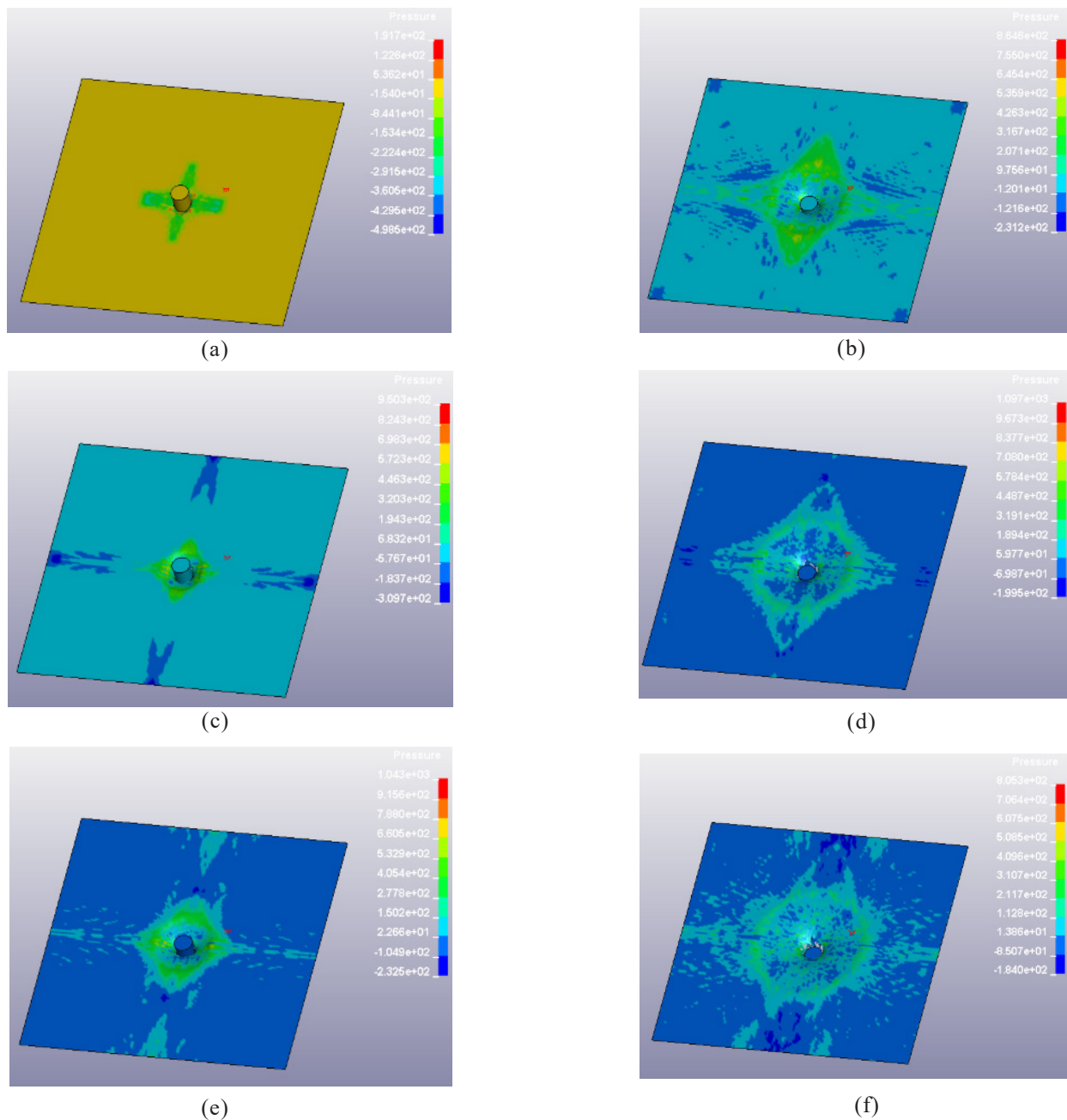


Figure 4. Variation of pressure distribution in UHMWPE plates over time, (a) $t = 0.0000148$ s; (b) $t = 0.0000599$ s; (c) $t = 0.0000299$ s; (d) $t = 0.000749$ s; (e) $t = 0.0000449$ s; and (f) $t = 0.000899$ s.

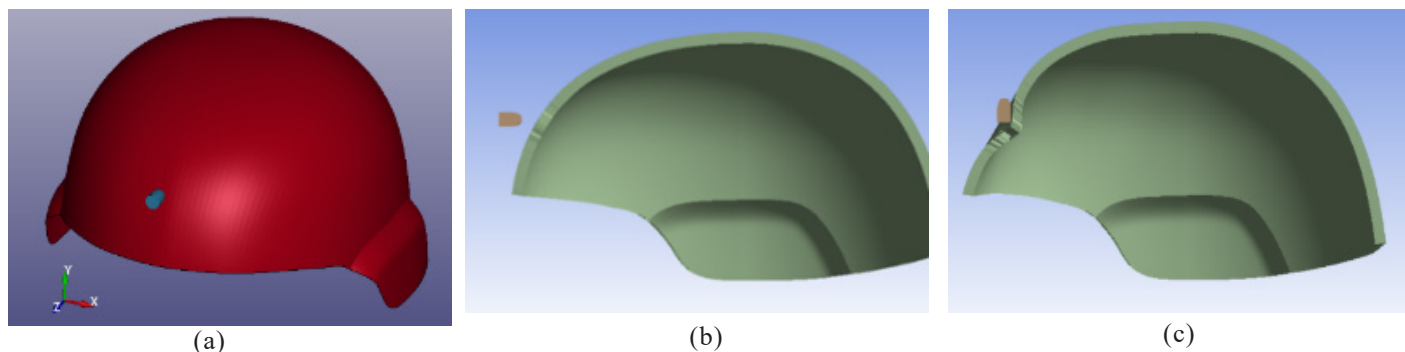


Figure 5. Position and coordinates of the helmet and the threat relative to each other, (a) Helmet coordinates; (b) Position 1; and (c) Position 2.

when the kinetic energy of the threat is exhausted. In this study, dynamic deformation is considered as back-face deformation.

3.3.1 Ballistic Performance of Kevlar Helmet

Ballistic helmets are modeled with 15 layers and 6.8 mm in thickness. The threat was fired directly into the frontal area of the ballistic helmet.

The firing conditions are shown in Fig. 5. The initial state of the threat and the moment of impact are shown in position 1 and position 2.

In ballistic tests where no damping elements were used, the dynamic deflection of the Kevlar helmet was measured to be 16.9 mm. Although a complete penetration did not occur, lateral damage was observed in the composite structure. Here, it is shown in Fig. 6 (a) that the damage progressing in the composite laminae shows tearing in the helmet axis. The helmet shell, which reached the stress and strain limits, showed separations on the equatorial axis.

The type of composite damage that occurred in the Kevlar helmet is very similar to the type of damage that occurred in the Kevlar helmets in previous studies. The area of permanent deformation is elliptical⁷. As shown in Fig. 6 (a), the thickness of the helmet decreases from 6.8 mm to 5.1 mm at the impact location and an even opening is observed. This situation can be considered as delamination as well as fibre and matrix damage. In the previous experimental and numerical model developed by Palta⁷, *et al.* 9 mm FMJ was fired into a Kevlar helmet and fibre and matrix damage as well as delaminations were observed at the impact site.

According to NIJ II standards, the over time pressure distributions in the Kevlar helmet after a ballistic shot are shown in Fig. 7(a). The sudden point pressure starting with the impact of the endpoint of the threat shows a distribution in the helmet geometry as the projectile advances. Until the energy of the projectile was exhausted, the pressure along the fibre axes in the helmet continued to disperse. After the projectile was stopped, the pressure in and around the impact zone decreased by spreading over the entire geometry. The instantaneous pressure generated here is point pressure and is distributed depending on the helmet geometry. Tearing and fibre-matrix damages were observed at the points where the pressure was maximum.

3.3.2 Ballistic Performance of UHMWPE Helmet

In this section, NIJ II level ballistic tests were simulated in a UHMWPE ballistic helmet with the same coordinate axis, geometry, number of layers, and thickness as the Kevlar helmet. UHMWPE is thermoplastic-based and is a very light and relatively soft material with strong fibers. The dynamic back face deformation of the UHMWPE helmet was measured as 18.8 mm after the shot. Crushing and deformation were observed.

As shown in Fig. 6(b), the thickness change in the UHMWPE helmet at the moment of the highest impact pressure is not as high as in the Kevlar helmet. The thinning of the composite at the impact location is around 0.1 mm. In addition to this crushing, back face deformation was measured.

According to NIJ II standards, the over time pressure distributions in the UHMWPE helmet after the ballistic shot are shown in Fig. 7(b). The sudden point pressure starting with the impact of the endpoint of the threat shows a distribution in the helmet geometry as the projectile advances. The pressure along the fibre axes in the helmet continued to distribute until the energy of the projectile was exhausted. After the projectile was stopped, the pressure in and around the impact zone decreased by spreading over the entire geometry. The UHMWPE helmet absorbed all the pressure and complete penetration was not observed. The maximum point pressure value is lower than the maximum pressure value of the Kevlar helmet.

3.3.3 Ballistic Performance Comparison of Kevlar and UHMWPE Helmet

As a result of the analysis, both Kevlar and UHMWPE helmets provided the required protection at the NIJ II level in the specified layer and thickness. Full penetration did not occur in both ballistic helmets. Dynamic back face deformation was slightly higher in the UHMWPE helmet than in the Kevlar helmet. The threat pushes the shell of the helmet until its energy is exhausted and stops pushing when its energy is exhausted. If this deformation occurs until the personnel's skull is impacted, it causes trauma. Table 6 shows the dynamic deflection causing the trauma.

It can be argued that the lower density and therefore lower weight of the UHMWPE helmet will provide a significant advantage to military personnel on the battlefield. Considering the densities, the UHMWPE helmet is 21.2 % lighter than a Kevlar helmet of the same volume. In addition, while fibre and matrix damage and composite segregation were observed in the Kevlar helmet, this was not observed in the UHMWPE helmet.

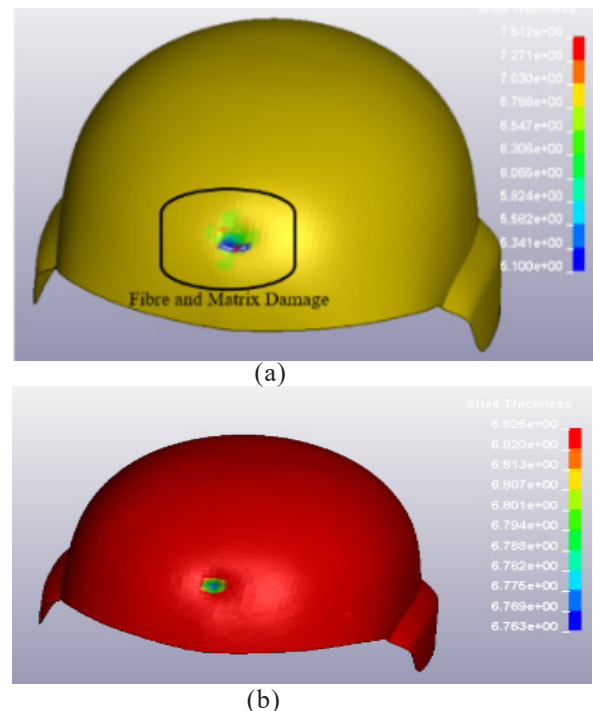


Figure 6. Composite damage on Kevlar and UHMWPE helmet after NIJ II test, (a) Kevlar helmet; and (b) UHMWPE helmet.

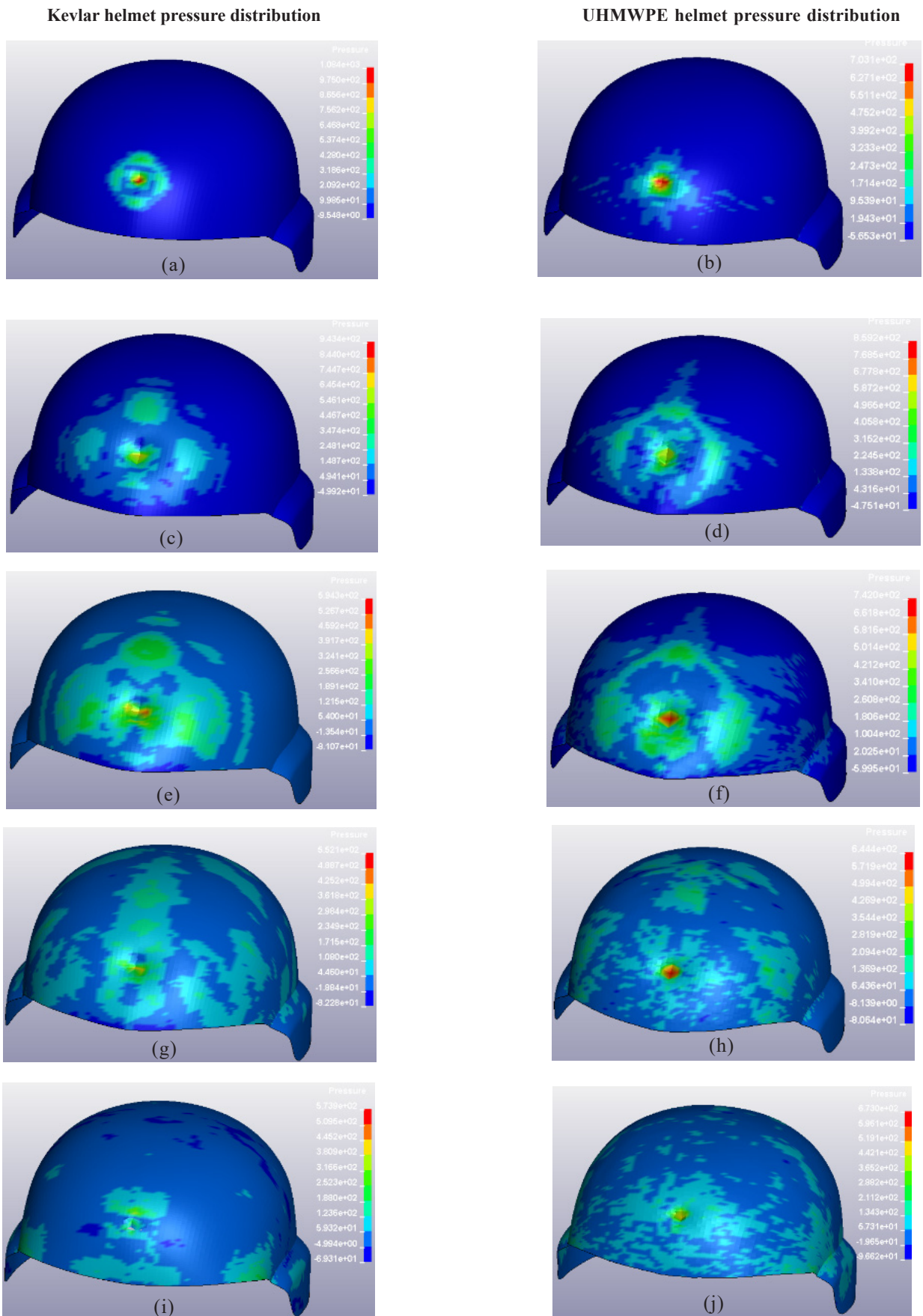


Figure 7. Variation of pressure distribution in a Kevlar and UHMWPE helmets over time, (a) $t = 0.0000449$ s; (b) $t = 0.0000449$ s; (c) $t = 0.0000899$ s; (d) $t = 0.0000899$ s; (e) $t = 0.0001199$ s; (f) $t = 0.0001199$ s; (g) $t = 0.0002$ s; (h) $t = 0.0002$ s; (i) $t = 0.0003$ s; and (j) $t = 0.0003$ s.

Table 6. Ballistic performance comparison of Kevlar and UHMWPE helmets

Helmets	Dynamic deflection (mm)	Complete penetration	Density (kg/m ³)
Kevlar helmet	16.9	NO	1230
UHMWPE helmet	18.8	NO	970

4. CONCLUSIONS

In this study, the ballistic performance and protection mechanisms of Kevlar and UHMWPE helmets at NIJ protection levels were analyzed and compared. Firstly, a ballistic limit determination study was carried out on the Kevlar plate according to STANAG standards with experimental data obtained from the literature. The results of the experimental study converged with a margin of error of 4.64 %. In the verification of the Kevlar model, 1.1 g of FSP was fired at 400×400×9.1 mm, 20-layer composites. The ballistic limit was found to be 720 ± 10 m/s.

In the verification of UHMWPE armour, convergence with a previously developed model was attempted. In the residual velocity determination simulations, 20 mm FSP was fired at a 300×300×10 mm plate. Convergence to the previous analytical model converged with an error of 1 %. The accuracy of the numerical models created within the scope of this study has been proved with the studies carried out on Kevlar and UHMWPE plates.

Ballistic helmets were modeled after sufficiently converging plate armour. At the NIJ II level, an 8 g FMJ threat was fired at 358 m/s into the front of the helmet. Dynamic deformation and composite damage were investigated in ballistic helmets. The pressure changes of both ballistic helmets over time were also calculated and presented in the literature. While 16.9 mm dynamic deformation occurred in the Kevlar helmet, geometry separation, fibre, and matrix damage were observed. In the UHMWPE helmet, the dynamic deformation was measured as 18.8 mm, but no composite damage was observed as in Kevlar. In conclusion, both ballistic helmets provide NIJ II levels of protection. However, the UHMWPE helmet is 21.2 % lighter than the Kevlar helmet due to its very low density and the absence of any observed separation, it can be concluded that it will be advantageous for military personnel on battlefields.

REFERENCES

- Li, Y.; Fan, H. & Gao, X.L. Ballistic helmets: Recent advances in materials, protection mechanisms, performance, and head injury mitigation. *Composites Part B: Engin.*, 2022, **238**, 109890. doi: 10.1016/j.compositesb.2022.109890
- Defense Medical Surveillance System (DMSS), Theater Medical Data Store (TMDS) provided by the Armed Forces Health Surveillance Division (AFHSD) Prepared by the Traumatic Brain Injury Center of Excellence (TBICoE) 2000–2021 Q2, as of August 26, 2021
- Mortlock, R.F. Protecting American soldiers: The development, testing, and fielding of the Enhanced Combat Helmet (Ech). *Project Manage. J.*, 2018, **49**(1), 96-109. doi: 10.1177/875697281804900107
- Baykara, T.; Günay, V.; Demirural, A. Armour Technology. Yeditepe University Press, Istanbul, 2020.
- Zhang, T.G.; Satapathy, S.S.; Vargas-Gonzalez, L.R. & Walsh, S.M. Ballistic impact response of ultra-high-molecular-weight polyethylene (UHMWPE). *Composite Struct.*, **133**, 2015, 191-201. doi: 10.1016/j.compstruct.2015.06.081
- Kulkarni, S.G.; Gao, X.L.; Horner, S.E.; Zheng, J.Q. & David, N.V. Ballistic helmets—their design, materials, and performance against traumatic brain injury. *Composite Struct.*, 2013, **101**, 313-331. doi: 10.1016/j.compstruct.2013.02.014
- Palta, E.; Fang, H. & Weggel, D.C. Finite element analysis of the Advanced Combat Helmet under various ballistic impacts. *Int. J. Impact Engin.*, 2018, **112**, 125-143. doi: 10.1016/j.ijimpeng.2017.10.010
- Rodríguez-Millán, M.; Ito, T.; Loya, J.A.; Olmedo, A. & Miguélez, M.H. Development of numerical model for ballistic resistance evaluation of combat helmet and experimental validation. *Materials & Design*, 2016, **110**, 391-403. doi: 10.1016/j.matdes.2016.08.015
- Aare, M. & Kleiven, S. Evaluation of head response to ballistic helmet impacts using the finite element method. *Int. J. Impact Engin.*, 2007, **34**(3), 596-608. doi:10.1016/j.ijimpeng.2005.08.001
- Hisley, D.M.; Gurganus, J.C. & Drysdale, A.W. Experimental methodology using digital image correlation to assess ballistic helmet blunt trauma. 2011. doi: 10.1115/1.4004332
- Palomar, M.; Lozano-Mínguez, E.; Rodríguez-Millán, M.; Miguélez, M.H. & Giner, E. Relevant factors in the design of composite ballistic helmets. *Composite Struct.*, 2018, **201**, 49-61. doi: 10.1016/j.compstruct.2018.05.076
- Sun, X.; Zhang, L.; Sun, Q.; Ye, P.; Hao, W.; Shi, P. & Dong, Y. Anti-penetration performance of composite structures with metal-packaged ceramic interlayer and UHMWPE Laminate. *Materials*, 2023, **16**(6), 2469. doi: 10.3390/ma16062469
- Mansoori, H. & Zakeri, M. Strain-rate-dependent progressive damage modelling of UHMWPE composite laminate subjected to impact loading. *Int. J. Damage Mech.*, 2022, **31**(2), 215-245. doi: 10.1177/10567895211035
- Lakshmana Rao, C.; Narayanamurthy; V. & Simha, K. *Appl. Impact Mech.*, 2016. doi: 10.1002/9781119241829
- A voluntary national standard promulgated by the National Institute of Justice Supersedes NILECJ-STD-0106.00 dated September 1975
- NATO Standardization Agency, STANAG 2920 PPS (ed 2) – Ballistic Test Method for Personal Armour Materials and Combat Clothing, 2003
- Mevlut, H. Functionally graded plates ballistic limits at different projectile impact angles investigation. *Erciyes*

University, Kayseri, Turkey, 2017. (MSc Thesis)

18. LS DYNA MANUEL VOL II 2012
19. Zhang, R.; Qiang, L.S.; Han, B.; Zhao, Z.Y.; Zhang, Q.C.; Ni, C.Y. & Lu, T.J. Ballistic performance of UHMWPE laminated plates and UHMWPE encapsulated aluminum structures: Numerical simulation. *Composite Struct.*, 2020, **252**, 112686.
doi: 10.1016/j.compstruct.2020.112686

ACKNOWLEDGMENT

This study was supported by the Scientific Research Projects Unit of Erciyes University (ERU/BAP) under the research Grant No: FBAÜ-2023-12517.

CONTRIBUTORS

Mr I.F. Saruhan continues his Master's degree in Mechanical Engineering at Erciyes University, Kayseri. He works at the CES advanced composite and defense technologies R&D office in Ankara. His research interests are mechanics of composite materials, numerical simulation, and ballistics. In the current study, he carried out CAD modeling and numerical simulation studies.

Prof Dr R. Gunes is a Professor at Erciyes University, Turkey. His research interests are mechanics of composite materials, numerical simulations, impact, and ballistics. He served as an academic advisor in the current study.